




# Permeability Measures Predict Hemorrhagic Transformation after Ischemic Stroke

Andrew Bivard, PhD,<sup>1</sup> Timothy Kleinig, PhD,<sup>2</sup> Leonid Churilov, PhD, FRACP,<sup>3</sup> Christopher Levi, FRACP,<sup>3</sup> Longting Lin, PhD ,<sup>4</sup> Xin Cheng, MD, PhD,<sup>5</sup> Chushuang Chen, PhD ,<sup>4</sup> Richard Aviv, FRACP,<sup>6</sup> Philip M. C. Choi, FRACP,<sup>7</sup> Neil J. Spratt, PhD, FRACP,<sup>4</sup> Kenneth Butcher, MD, PhD, FRCP(C), FRACP ,<sup>8</sup> Qiang Dong, MD, PhD,<sup>5</sup> and Mark Parsons, PhD, FRACP<sup>1</sup>

**Objective:** We sought to examine the diagnostic utility of existing predictors of any hemorrhagic transformation (HT) and compare them with new perfusion imaging permeability measures in ischemic stroke patients receiving alteplase only.

**Methods:** A pixel-based analysis of pretreatment CT perfusion (CTP) was undertaken to define the optimal CTP permeability thresholds to predict the likelihood of HT. We then compared previously proposed predictors of HT using regression analyses and receiver operating characteristic curve analysis to produce an area under the curve (AUC). We compared AUCs using  $\chi^2$  analysis.

**Results:** From 5 centers, 1,407 patients were included in this study; of these, 282 had HT. The cohort was split into a derivation cohort (1,025, 70% patients) and a validation cohort (382 patients or 30%). The extraction fraction (E) permeability map at a threshold of 30% relative to contralateral had the highest AUC at predicting any HT (derivation AUC 0.85, 95% confidence interval [CI], 0.79–0.91; validation AUC 0.84, 95% CI 0.77–0.91). The AUC improved when permeability was assessed within the acute perfusion lesion for the E maps at a threshold of 30% (derivation AUC 0.91, 95% CI 0.86–0.95; validation AUC 0.89, 95% CI 0.86–0.95). Previously proposed associations with HT and parenchymal hematoma showed lower AUC values than the permeability measure.

**Interpretation:** In this large multicenter study, we have validated a highly accurate measure of HT prediction. This measure might be useful in clinical practice to predict hemorrhagic transformation in ischemic stroke patients before receiving alteplase alone.

ANN NEUROL 2020;88:466–476

## Introduction

Symptomatic intracranial hemorrhage or hemorrhagic transformation (HT) occurs spontaneously after ischemic stroke. There are few useful predictive markers in clinical practice to identify which patients are at the highest risk

of HT. HT ranges from hemorrhagic infarction (HI), which may be a marker of successful reperfusion with minimal or no clinical impact,<sup>1</sup> to large parenchymal hematoma (PH), which substantially increases the risk of poor outcome, including death.<sup>2</sup> Treatment with alteplase

View this article online at [wileyonlinelibrary.com](http://wileyonlinelibrary.com). DOI: 10.1002/ana.25785

Received Aug 28, 2019, and in revised form May 13, 2020. Accepted for publication May 14, 2020.

Address correspondence to Prof Andrew Bivard, Departments of Neurology, Royal Melbourne Hospital, Parkville, VIC 3050, Australia. E-mail: [abivard@unimelb.edu.au](mailto:abivard@unimelb.edu.au)

From the <sup>1</sup>Departments of Neurology, Royal Melbourne Hospital, University of Melbourne, Melbourne, Victoria, Australia; <sup>2</sup>Department of Neurology, Royal Adelaide Hospital, Adelaide, South Australia, Australia; <sup>3</sup>Melbourne Medical School, University of Melbourne, Victoria, Australia; <sup>4</sup>Departments of Neurology, John Hunter Hospital, University of Newcastle, Newcastle, New South Wales, Australia; <sup>5</sup>Department of Neurology, Huashan Hospital, Fudan University, Shanghai, China; <sup>6</sup>Department of Radiology, Neuroradiology section, The Ottawa Hospital, Ottawa, Ontario, Canada; <sup>7</sup>Department of Neuroscience, Eastern Health, Eastern Health Clinical School, Faculty of Medicine, Nursing and Health Sciences, Monash University, Melbourne, Victoria, Australia; and <sup>8</sup>Department of Neurology, Department of Medicine, University of New South Wales, Kensington, New South Wales, Australia

is associated with a substantially increased risk of HT from 2.4 to 27%,<sup>3</sup> but this risk is balanced against a higher chance of improved clinical outcomes in appropriately selected patients.<sup>4–6</sup> A means of accurately predicting which patients may or may not be at risk of PH or symptomatic intracranial hemorrhage could have significant clinical implications and better inform the treatment decision-making process.

Vascular permeability can be measured with magnetic resonance imaging (MRI) or computed tomography perfusion (CTP)<sup>7</sup> by measuring the rate of contrast leaving a voxel, with the assumption being that a slower or reduced contrast outflow (compared with inflow) is attributable to elevated blood vessel permeability. Elevated permeability may represent disruption or “leakiness” of the blood–brain barrier (BBB), where contrast becomes trapped in the BBB or leaks into the surrounding tissue. Permeability is quantified by analysis of dynamic contrast-enhanced images (unprocessed perfusion imaging maps showing contrast flow) to observe decreases in hydrostatic gradients between blood vessels and brain tissue, which can result in contrast lingering around blood vessels. Permeability measures reflect a complex interaction between several physiological variables that affect contrast leakage, such as edema, mass effect, transmural pressure, interstitial fluid pressure, and abnormal tissue biomechanical properties related to BBB permeability. For example, tissue blood volume is associated with abnormal BBB permeability, and several studies have observed a link between decreased cerebral blood volume (CBV) and increased BBB permeability. This is relevant because CBV has been proposed as a marker of increased hemorrhage risk. Permeability maps generated from magnetic resonance perfusion-weighted imaging (PWI) and computed tomography perfusion (CTP) have previously been proposed as measures to predict HT<sup>8,9</sup> owing to the proposed relation between permeability maps and blood vessel integrity. However, the accuracy or clinical usefulness of permeability imaging is not yet clear, and there are multiple permutations of permeability measures.<sup>10</sup> However, there is evidence suggesting that BBB permeability<sup>11,12</sup> can increase in the first few hours after stroke and that elevated permeability measured on CTP might indicate ischemia-induced vascular damage<sup>13</sup> and serve as a marker to predict HT.<sup>14</sup>

Previous studies have identified a plethora of clinical risk factors for HT, including advancing age, stroke severity, pretreatment hypertension, and concurrent use of antithrombotic agents. In addition, other studies have identified imaging and laboratory markers, such as hyperglycemia, thrombocytopenia, extensive early ischemic changes on computed tomography (CT), the hyperdense middle cerebral artery sign, very low cerebral blood flow

lesion volume, severely delayed blood flow, and large ischemic core volume, which have been related to HT events.<sup>15–18</sup> However, apart perhaps from major early ischemic change (which is a poor prognostic marker irrespective of HT), none as yet has translated into clinical practice as a routinely used predictor of hemorrhagic transformation. In the present study, we sought to assess the diagnostic utility and association of permeability measures acquired with acute CTP and to identify the optimal cut points for HT outcome in ischemic stroke patients. Next, we sought to compare previously proposed markers of HT with CTP permeability imaging and to assess the comparative accuracies in a large multicenter dataset. We hypothesised that permeability imaging would be an accurate measure of HT of equal or greater value to other validated markers of HT prediction.

## Patients and Methods

Consecutive acute ischemic stroke patients presenting to hospital within 4.5 hours of symptom onset at 5 centers (John Hunter Hospital, New South Wales, Australia; Box Hill Hospital, Melbourne, Victoria, Australia; Royal Adelaide Hospital, Adelaide, South Australia, Australia; Huashan Hospital, Shanghai, China; and Sunnybrook Health Science Centre, Toronto, Ontario, Canada) between 2011 and 2016 were recruited prospectively for the INternational Stroke Perfusion Imaging REgistry (INSPIRE). As part of the registry, patients underwent baseline multimodal CT imaging with non-contrast CT, CTP, and follow-up imaging with MRI or CT at 24 hours post-stroke. Clinical stroke severity was assessed at the two imaging time points using the National Institutes of Health Stroke Scale (NIHSS). All patients in this study were treated with intravenous thrombolysis according to local guidelines and at the clinical judgement of the treating physician. The modified Rankin scale (mRS) was assessed 90 days after stroke. Thrombectomy cases were excluded from this study. Written informed consent was obtained from all participants, and the INSPIRE study was approved by the local ethics committees.

## Acute Multimodal CT Protocol

Participants recruited at John Hunter Hospital and Royal Adelaide Hospital were scanned using a Toshiba Aquilion 320-slice CT scanner (Toshiba Medical Systems, Tokyo, Japan). A total of 19 acquisitions occurred in 60 seconds. Forty milliliters of contrast agent (Ultravist 370; Bayer HealthCare, Berlin, Germany) was injected at 6ml/s, followed by 30ml of saline. Participants recruited at Box Hill Hospital were scanned using a 64-detector GE lightspeed (GE Healthcare, Waukesha, WI). A total of

19 acquisitions occurred in 54 seconds. Forty-five milliliters of contrast agent (Ultravist 370; Bayer HealthCare, Berlin, Germany) was injected at 6ml/s. Participants recruited at Huashan Hospital were scanned using a Brilliance iCT 126-slice CT scanner (Philips Medical Systems, Cleveland, OH). A total of 23 acquisitions occurred in 60 seconds. Forty milliliters of the same contrast was injected at 5ml/s, followed by 20ml of saline. Participants recruited at Sunnybrook Health Sciences Center underwent an acute CT with a 64-row CT scanner (GE Healthcare, Waukesha, WI). Baseline and 24 hour CT angiogram parameters were as follows: 0.7ml/kg iodinated contrast agent up to a maximum of 90ml (Omnipaque 300mg iodine/ml; GE Healthcare, Piscataway, NJ); 5–10 second delay; 120kVp; 270mA; rotation, 1 second; 1.25-mm-thick sections; table speed, 20.62mm per rotation. Biphasic CT perfusion protocol from basal ganglia to the lateral ventricles: 80kVp; 150mA; collimation, 8 × 5 mm; rotation, 1 second for 45 seconds followed by 6 further acquisitions 15 seconds apart for a total of 135 seconds. Iodinated contrast agent 0.5ml/kg (maximum 50ml) at 4ml/s was administered 5 seconds before the start of the sequence. All acute perfusion imaging acquired 60mm or more of coverage.

### Twenty-four Hour Imaging Protocol

As close as possible to 24 hours after acute imaging, all patients, regardless of treatment, underwent a stroke MRI protocol on a 1.5 or 3T scanner (Siemens Avanto or Verio). The magnetic resonance (MR) protocol included: diffusion-weighted imaging (DWI), perfusion-weighted imaging (PWI), MR time-of-flight angiography (MRA), and fluid-attenuated inversion recovery (FLAIR) imaging. For those with a contraindication to MRI, repeat non-contrast CT (NCCT) and CTP was performed using the above protocols.

### Imaging Analysis

All perfusion imaging was post-processed with the commercial software MISTar (Apollo Medical Imaging Technology, Melbourne, Victoria, Australia). Acute perfusion imaging was processed using single value deconvolution with delay and dispersion correction.<sup>19</sup> Areas of no blood flow, chronic infarction or cerebrospinal fluid regions were masked from the perfusion maps. Pixels with no blood flow were removed by eliminating areas where cerebral blood flow = 0, and cerebrospinal fluid/ventricle and skull pixels were removed using a Hounsfield unit threshold and geometric analysis. Previously validated thresholds were applied in order to measure the volume of the acute perfusion lesion (relative delay time [DT] >3 seconds) and

acute ischemic core (relative cerebral blood flow [CBF] <30%).<sup>20</sup> Penumbra volume was calculated as the volume of the perfusion deficit (DT threshold >3 seconds) minus the volume of the ischemic core (relative CBF threshold <30% within the DT >3 seconds lesion). The volume of severely hypoperfused tissue (Tmax >14 seconds)<sup>21</sup> and very low CBV (defined as <2.5th percentile of brain contralateral to the infarct)<sup>22</sup> was also recorded for use in HT prediction models.

The 24 hour follow-up MRI and/or CT scans were read and Heidelberg Bleeding Classification subtypes categorised by 2 raters (A.B. and M.P.), with any disagreement resolved by a third reader (C.L.). Raters were blinded to all the other imaging and clinical data. Reviewers were blinded to all other imaging. The presence or absence of post-thrombolytic bleeding was then ascertained on 24 hour imaging. Patients were then divided into a target group (HT evident) and a negative HT group. The raters categorised HT in the HT evident group into eight subtypes based on Heidelberg Bleeding Classification as: (1<sub>a</sub>) for hemorrhagic infarction 1 (HI1), scattered small petechiae, no mass effect; (1<sub>b</sub>) for HI2, confluent petechiae, no mass effect; (1<sub>c</sub>) for parenchymal hemorrhage 1 (PH1), hematoma within infarcted tissue, occupying <30%, no substantive mass effect; (2) for PH2, hematoma occupying ≥30% of the infarcted tissue, with obvious mass effect; (3<sub>a</sub>) for parenchymal hematoma remote from infarcted brain tissue; (3<sub>b</sub>) for intraventricular hemorrhage; (3<sub>c</sub>) for subarachnoid hemorrhage; and (3<sub>d</sub>) for subdural hemorrhage.<sup>23</sup>

### Permeability Measures

All permeability measures were performed using MISTar, and for each patient three permeability maps were generated. The extraction fraction ( $E$ ) was calculated as the fraction of contrast agent removed from the tissue contrast enhancement curve or input residue function during the first pass. At  $t_1$ , the unextracted tracer exits via outflowing blood, and the detector response registers the fraction of extracted tracer, given by  $E$ . After  $t_1$ , the extracted tracer diffuses back into the blood and is cleared by outflowing blood, giving rise to a gradually decreasing parenchymal phase. The parameters that can be obtained directly from fitting experimental curves  $t_1$  are the rate of transfer from intravascular to extravascular compartment ( $k_{21}$ ) and rate of transfer from extravascular to intravascular compartment ( $k_{12}$ ). Formally,  $E$  can be given by:

$$E = 1 - e^{-k_{21}t_1}$$

which is a function of the vascular transit time,  $t_1$ . This expression for  $E$  implies that, for two capillaries with the same outflow (extravasation) rate,  $k_{21}$ , the fraction of tracer extracted in the first pass would be larger for the capillary with the longer transit time.<sup>24–26</sup> The permeability–surface area product ( $P \times S$ , often written  $PS$ ) is the flow of molecules through the capillary membranes in a certain volume of tissue (expressed in milliliters per minute per 100ml tissue).  $PS$  depends not only on the characteristics of the capillary wall, but also on the contrast agent used.  $PS$  represents the total diffusional flux across all capillaries and is measured in milliliters per minute per 100g of tissue. It can be interpreted as follows: the unidirectional flux of solutes from blood plasma to the interstitial space is equivalent to the complete transfer of all the solutes in  $PS$  milliliters of blood per minute to the interstitial space. In the normal brain parenchyma, BBB is intact and tightly regulated.  $PS$  is normally 0 for large hydrophilic molecules, such as a peripherally injected iodinated contrast agent.  $PS$  is sometimes called  $K_{trans}$ , but  $PS$  corresponds to  $K_{trans}$  only in very specific conditions. The assumption that back-flux from extravascular compartment into the intravascular one can be neglected during early times depends on the relative magnitude of blood flow ( $F$ ) and the capillary  $PS$ . Permeability ( $P$ ) is related to the diffusion coefficient of contrast agent in the pores of the capillary endothelium, which are assumed to be water filled. The diffusion flux of contrast agent across the capillary endothelium is dependent on both the diffusion coefficient and the total surface area of the pores or the  $PS$  product. The  $PS$  product has the same dimensions as  $F$ , and thus the ratio  $PS/F$  is dimensionless.  $PS$  is related to  $K$  as follows:

$$K = EF$$

If  $PS/F < 1$ , then  $K \approx PS$ . In normal cerebral vasculature,  $PS$  is negligible for all contrast agents presently in use. The relative magnitude of  $PS$  and  $F$  also determines  $E$ .<sup>27,28</sup> In summary,  $E$  is the ratio of contrast leaving a voxel, as opposed to measures such as CBF or CBV, which measure contrast inflow.

The transfer constant,  $K_{trans}$ , is a complex combination of tissue blood flow and  $PS$  in varying proportions, as follows:

$$K_{ep} = \frac{1}{(TTP_{tissue} - TTP_{plasma})}$$

$$K_{trans} = V_e \times K_{ep}$$

$$V_e = \frac{C_{tissue}}{C_{plasma}}$$

where  $C_{tissue}$  is the concentration of contrast in the tissue,  $C_{plasma}$  the concentration of contrast in the plasma,  $TTP_{tissue}$  the time to reach the peak intensity value in the tissue, and  $TTP_{plasma}$  is the time to reach the peak intensity in the plasma in the time–intensity graph for tissue and plasma, respectively.<sup>12</sup>

## Permeability Analysis

For each of the three “types” of the maps defined above ( $E$ ,  $K_{trans}$  and  $PS$ ), a voxel-based analysis was performed, initially with a whole-hemisphere region of interest and subsequently with the region of interest constrained within the perfusion lesion to define the “location” class (set as a threshold of DT >3 seconds). This results in six individual classes per patient that combine “type” and “location”. For each of these six classes individually, a relative threshold at 5% increments (range 0–100%) was tested, resulting in 20 threshold-specific maps (120 maps overall per patient).

Threshold-based analysis: In order to identify the optimal threshold to predict HT, for each of the 120 threshold-specific maps a receiver operating characteristic (ROC) curve analysis was used to test the predictive performance of CTP permeability maps at predicting hemorrhagic outcome for: (1) all HT; (2) only HI; (3) only PH (PH1 and PH2); and (4) remote hemorrhage. Results are presented as an area under the curve (AUC) with 95% confidence intervals (CIs) for the whole ROC curve for a perfusion map at a single threshold. Specificity, sensitivity, positive predictive value, and negative predictive value were calculated for each threshold increment (eg,  $E$ ,  $K_{trans}$ , and  $PS$ ). The optimal thresholds were determined by the highest AUC. All CTP scans with an acquisition or contrast curve (time from the start of the signal increase attributable to contrast arrival) of <45 seconds were excluded from this study owing to the inability to measure  $K_{trans}$  and  $PS$  accurately from these scans.

## Statistical Analysis

Statistical analyses were programmed using Stata v.13.0 (StataCorp Ltd, College Station, TX). Descriptive results and quantitative baseline patient characteristics were presented as the mean  $\pm$  standard deviation (SD) or the median and interquartile range. Student paired  $t$  tests or Wilcoxon signed-rank tests were performed for parametric or nonparametric data, respectively.

The study cohort was split into derivation and validation cohorts for analysis (70 and 30%, respectively), using stratified sampling to ensure that there were no significant differences between the cohorts in terms of baseline characteristics or the occurrences of HT/PH.

An ROC curve analysis was used to estimate the AUC, sensitivity, and specificity of each of the permeability maps as a prognostic tool for hemorrhagic outcome. In the ROC analysis, each measurement threshold is a whole analysis and not a point on an ROC curve. Next, an analysis was undertaken to identify whether there was a relation between the volume of the permeability lesion and the Heidelberg HT grade, using ordinal logistic regression. Additionally, patients were analyzed separately based the location of the hemorrhage (either around the area of follow-up infarction or remote from the initial ischemia on CTP). Lastly, once derived, the optimal permeability measure was again assessed within the validation cohort using ROC AUC analysis. The validation ROC AUC values are compared between the pre-specified threshold values to identify the potentially optimal threshold using  $\chi^2$  analysis.

Once the optimal cut points to predict HT grade were determined, a further ROC AUC analysis was performed using previously identified markers of HT grade (ischemic core volume, very low CBV, Tmax + 14 second volume, reperfusion, diabetes, and age) and compared with the optimal permeability AUC using  $\chi^2$  analysis.

## Results

Throughout the study period, the INSPIRE registry collected 2,127 patients who underwent acute CTP imaging

within 4.5 hours of symptom onset and were treated with intravenous alteplase. From the cohort of 2,127 patients, a total of 317 were excluded from the study analysis: 154 because they had incomplete clinical data, and 93 because the imaging could not be processed owing to excessive motion or other technical errors. A further 203 patients were excluded because their acquisition time was <45 seconds. Of the remaining 1,407 patients, 282 developed HTs (91 HI1/1<sub>a</sub>, 107 HI2/1<sub>b</sub>, 51 PH1/1<sub>c</sub>, and 33 PH2/2, 29 of which were symptomatic). Additionally, of the 282 HTs, 47 were 3<sub>a,b,c</sub> remote from the infarct and 235 were involving the infarct. The cohort of 1,407 patients were then split into derivation (1,025 patients, 197 HTs) and validation (382 patients, 85 HTs) cohorts for subsequent analysis. Lastly, of the included patients, 493 had follow-up MRI rather than CT (77 HTs, 26 HI1/1<sub>a</sub>, 11 HI2/1<sub>b</sub>, 23 PH1/1<sub>c</sub>, and 17 PH2/2).

The baseline characteristics of patients are listed in Table 1. There were significant differences between the baseline NIHSS, baseline perfusion lesion volume, baseline ischemic core volume, and treatment types between patients with and without any HT at 24 hours. There were also significant differences in the 24 hour NIHSS, 3 month mRS, and 24 hour core volume between patients with and without any HT at 24 hours (Table 1). There were no significant differences in the baseline characteristics between the derivation and validation cohorts ( $p > 0.05$ ).

**TABLE 1. Patient Clinical and Imaging Characteristics**

Characteristic	HT, n = 282 (mean, SD)	Non-HT, n = 1,125 (mean, SD)	<i>p</i>
Age (yr)	66 (15)	67 (13)	0.422
Time to scanning (min)	105 (49)	99 (51)	0.481
Baseline NIHSS	14 (6)	8 (5)	<0.001
Baseline perfusion lesion volume (DT3) (ml)	94 (69)	78 (65)	0.011
Baseline ischemic core volume (CBF 30%) (ml)	42 (43)	22 (17)	<0.001
Very low CBV (ml)	6 (9)	3 (7)	0.163
Tmax 14 s volume (ml)	23 (33)	15 (24)	0.107
24 h NIHSS	12 (8)	8 (7)	<0.001
90 day mRS	3 (1)	2 (1)	<0.001
24 h core volume: all patients (ml)	56 (42)	27 (18)	<0.001
24 h core volume: MRI follow-up patients (ml)	38 (21)	19 (11)	0.033

The baseline demographic information was compared between patients with and without a hemorrhagic transformation at 24 h. There were significant differences between the baseline NIHSS, baseline perfusion lesion volume, baseline ischemic core volume, and treatments. There were also significant differences in the 24 h NIHSS, 3 mo mRS, and 24 h core volume between study groups. All study patients were treated with intravenous alteplase. CBF = cerebral blood flow; CBV = cerebral blood volume; mRS = modified Rankin scale; NIHSS = National Institutes of Health Stroke Scale.

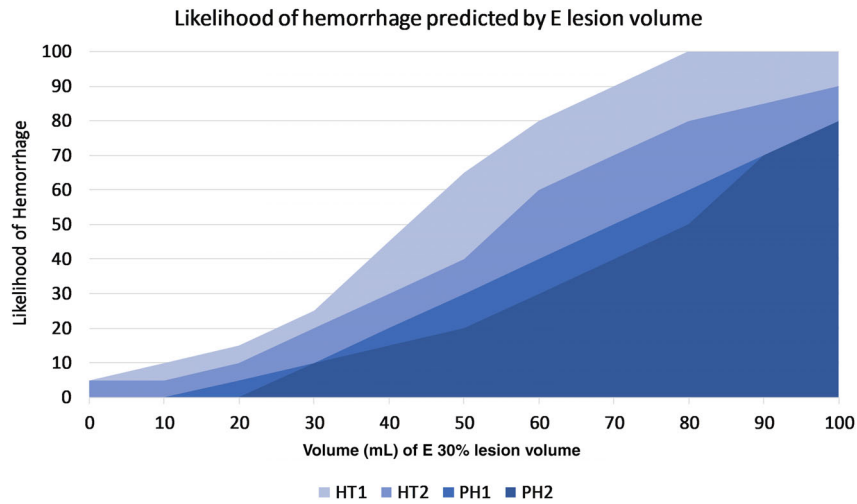
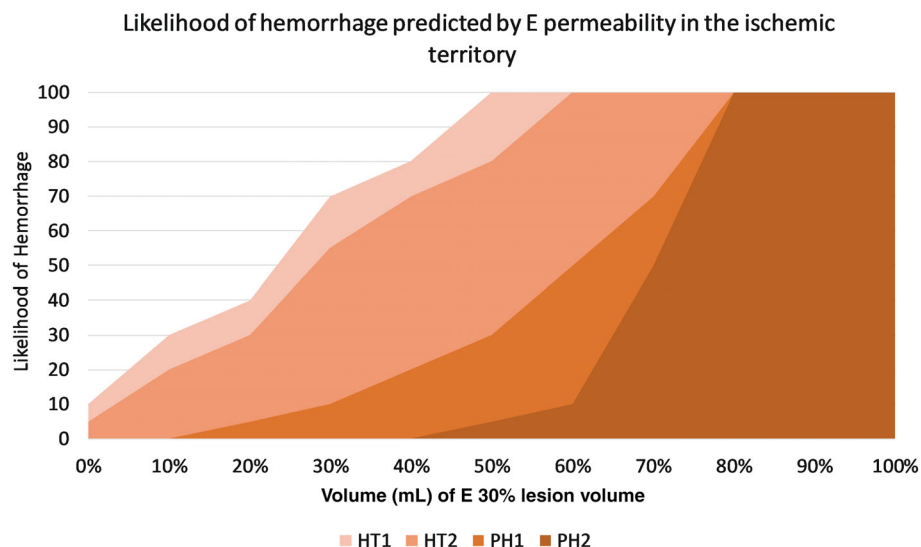


FIGURE 1: The likelihood of hemorrhagic transformation with the absolute *E* lesion volume. With increasing *E* lesion volume, there was an increased likelihood of hemorrhage and an increase in the severity of hemorrhage.

TABLE 2. Area Under the Curve and Sensitivity and Specificity Analysis of Permeability Measures for Predicting Hemorrhagic Transformation

Map	Threshold (%)	Derivation AUC	Sensitivity	Specificity	Positive predictive value (%)	Validation AUC	$\chi^2 p$
Whole-brain analysis							
<i>E</i>	20	0.82	0.86	0.79	76	0.79	0.067
	25	0.84	0.84	0.83	79	0.82	0.187
	30	0.85	0.93	0.78	81	0.84	0.038
	35	0.83	0.79	0.88	80	0.83	0.073
<i>PS</i>	60	0.74	0.42	0.77	66	<0.7	0.277
	65	0.73	0.43	0.68	68	<0.7	0.437
	70	0.73	0.32	0.77	71	<0.7	0.394
<i>K<sub>trans</sub></i>	65	0.74	0.40	0.82	51	<0.7	0.299
	70	0.71	0.47	0.85	58	<0.7	0.424
Analysis confined to within the perfusion lesion							
<i>E</i>	20	0.89	0.88	0.93	81	0.86	<0.001
	25	0.89	0.90	0.93	87	0.86	<0.001
	30	0.91	0.90	0.95	91	0.89	<0.001
	35	0.88	0.89	0.87	86	0.87	0.031
<i>PS</i>	60	0.71	0.34	0.55	76	0.67	0.387
	65	0.70	0.47	0.83	78	0.59	0.211
	70	0.73	0.34	0.82	80	0.64	0.347
<i>K<sub>trans</sub></i>	65	0.75	0.40	0.79	42	0.68	0.427
	70	0.74	0.54	0.83	55	0.66	0.447

Each AUC represents the result for the specific threshold tested. The  $\chi^2 p$  value represents the comparison between different thresholds. AUC = area under the curve.



**FIGURE 2:** The likelihood of hemorrhagic transformation with the absolute  $E$  lesion volume restricted to the perfusion lesion (DT3 seconds). With the increasing ratio of  $E$  lesion volume to perfusion lesion volume, there was an increased likelihood of hemorrhage and an increase in the severity of hemorrhage. The overall accuracy of the predictive model was high and more reliable than absolute  $E$  lesion volume alone. However, it was unusual for an individual patient to have a whole perfusion lesion permeability  $E$  30% lesion, and the results here represent data from a fitted risk model and represent associations rather than true individual patient risk.

The  $E$  permeability map of the whole brain at a threshold of 30% had the highest AUC for predicting any HT (derivation AUC 0.85, 95% CI 0.79–0.91; validation AUC 0.84, 95% CI 0.77–0.91; Fig 1 and Table 2). Additionally, an  $E$  permeability map of the whole brain at a threshold of 20% was also a reasonably strong predictor of HT (derivation AUC 0.82, 95% CI 0.76–0.88; validation AUC 0.79). Both the  $PS$  and  $K_{trans}$  maps of the whole brain were relatively poor predictors of HT overall ( $PS$  AUC 0.62, validation AUC 0.64;  $K_{trans}$  AUC 0.67, validation AUC 0.63). Importantly, permeability maps from  $E$ ,  $K_{trans}$ , or  $PS$  were not able to predict remote hemorrhage outside of the acute perfusion lesion in the ipsilesional or contralesional hemisphere (derivation and validation  $p > 0.5$ ), and remote hemorrhages were excluded from subsequent analyses. These results were maintained in the cohort of patients with MRI at follow-up ( $E$  permeability 30%, AUC 0.83, 95% CI 0.76–0.92;  $K_{trans}$  AUC <0.6,  $p > 0.5$ ;  $PS$  AUC <0.6,  $p > 0.5$ ).

There was an improved AUC for predicting HT when permeability was restricted to the perfusion lesion (with a threshold of DT >3 seconds) for the  $E$  maps at thresholds of 30% (derivation AUC 0.91, 95% CI 0.86–0.95; validation AUC 0.89, 95% CI 0.86–0.95; Fig 2 and Table 2) and 20% (derivation AUC 0.89, 95% CI 0.83–0.95; validation AUC 0.86). Lastly,  $E$  permeability maps at a threshold of 30% within the perfusion lesion were also very accurate at predicting patients with PH1/1<sub>c</sub> or PH2/2 (derivation AUC 0.93, 95% CI

0.89–0.96; validation AUC 0.9), whereas the  $K_{trans}$  and  $PS$  were relatively poor ( $PS$  AUC 0.67, validation AUC 0.68;  $K_{trans}$  AUC 0.66, validation AUC 0.64). An  $E$  map at a threshold of 30% within the perfusion lesion had the highest overall AUC at predicting HT across all tested measures (Table 2). Again these results were maintained in the cohort of patients with MRI at follow-up ( $E$  permeability 30%, AUC 0.89, 95% CI 0.78–0.96;  $K_{trans}$  AUC <0.6,  $p > 0.5$ ;  $PS$  AUC <0.6,  $p > 0.5$ ).

There was a significant association between the volume of the  $E$  permeability map deficit at a threshold of 30% and the severity of the hemorrhagic outcome, with every 10ml increase resulting in an increased chance of a higher grade of hemorrhagic outcome on an ordinal scale (odds ratio 1.13, 95% CI 1.08–1.43,  $p < 0.001$ ). Moreover, for every 1% increase in the volume of the  $E$  map 30% threshold lesion within the perfusion lesion, there was a 1% increase in the likelihood of a PH1/1<sub>c</sub> or PH2/2 (odds ratio, 2.01 95% CI 1.83–4.29,  $p < 0.001$ ). Neither  $K_{trans}$  nor  $PS$  volumes predicted PH1/1<sub>c</sub> or PH2/2 ( $p > 0.1$ ). For example, if a patient had an  $E > 30\%$  lesion volume that occupied >50% of the perfusion lesion, the likelihood of PH1/1<sub>c</sub> was 40% (sensitivity 0.87, specificity 0.81) and that of PH2/2 5% (sensitivity 0.75, specificity 0.83), whereas if only 70% of the perfusion lesion was occupied, the likelihood of PH1/1<sub>c</sub> was 70% (sensitivity 0.84, specificity 0.76) and that of PH2/2 50% (sensitivity 0.78, specificity 0.86). However, this result was not maintained in the MRI-



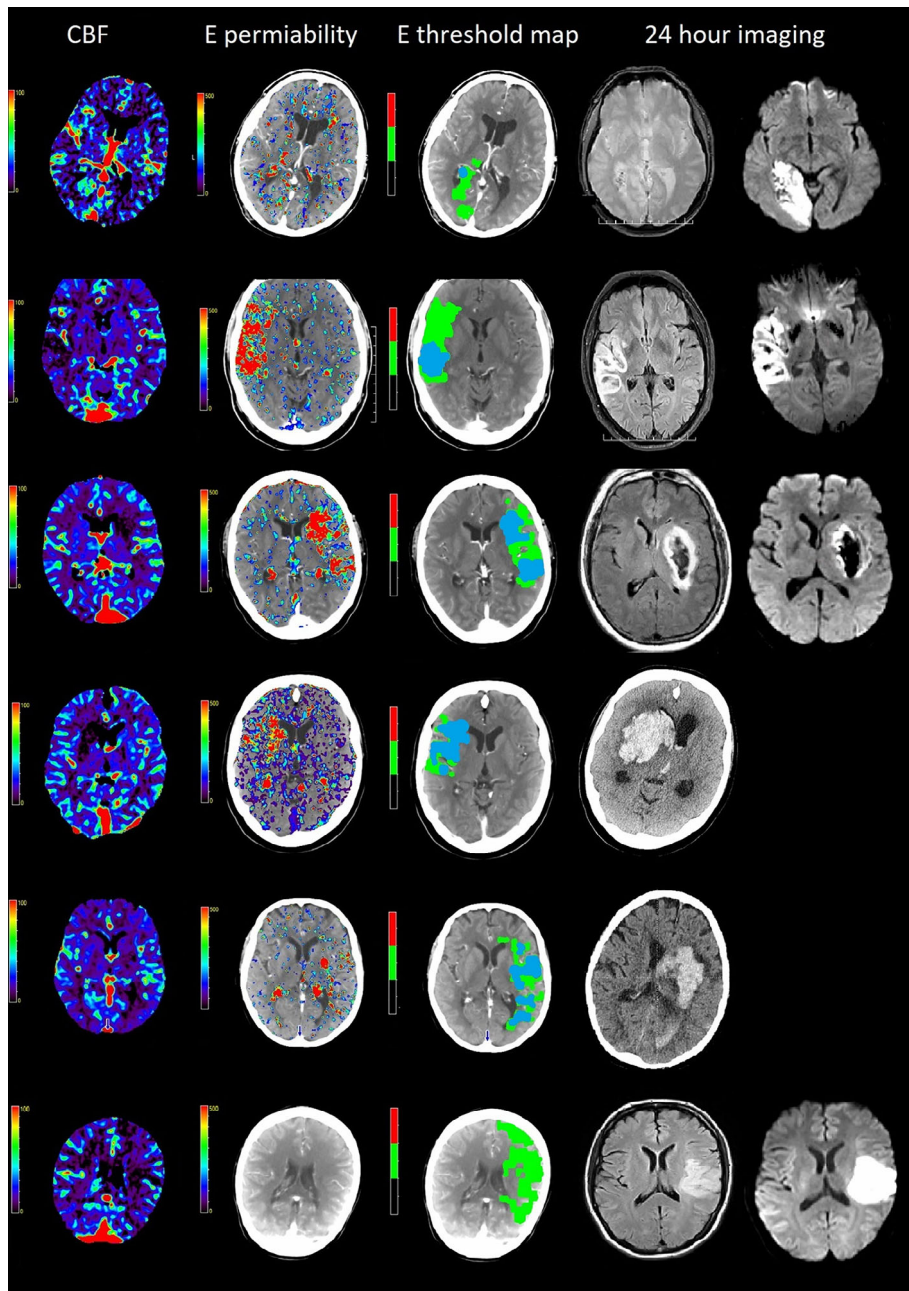


FIGURE 3: An example of the *E* permeability map output (2nd column) and a threshold *E* permeable map constrained within the perfusion lesion (3rd column), compared with a CTP CBF map (1st column), and the 24 hour CT/MRI (4th and 5th columns). On the *E* permeability map, the red represents a very prolonged contrast signal, suggesting high permeability. In the threshold map from the 3rd column, the blue area represents the *E* permeability >30% measure within the perfusion lesion (DT >3 seconds or Tmax >6 seconds). The ability of the *E* permeability maps to predict HT was significantly increased when a threshold was set at 30% and the lesion volume limited as a fraction of the perfusion lesion. In the first row, there is a small *E* permeability lesion, which predicted an HI1. The second row has a larger permeability lesion, but after a threshold was applied the fraction of permeability compared with the perfusion lesion was small, and only HI2 was predicted. Next, in the 3rd row, a denser permeability lesion is present, but again the volume was small and an HT2 was predicted. In the 4th row, there is a large, severe permeability lesion, and the patient went on to have a PH2. In the 5th row, the patient has a large perfusion lesion and large permeability lesion area, which developed into a PH2. The last row is an example of a patient with no permeability lesion despite a large perfusion lesion and no HT. CBF = cerebral blood flow; CT = computed tomography; CTP = CT perfusion; DT = delay time; *E*, extraction fraction; HI = hemorrhagic infarction; HT = hemorrhagic transformation; MRI = magnetic resonance imaging; PH = parenchymal hematoma.



only cohort (odds ratio 1.95 95%, CI 0.83–4.29,  $p = 0.427$ ).

In comparison to previously reported predictors of HT, permeability derived from an  $E$  map at a threshold of 30% (AUC 0.91,  $R^2 = 0.411$ ,  $p < 0.001$ , Fig 3) was a stronger predictor than ischemic core volume (AUC 0.62,  $R^2 = 0.341$ ,  $p = 0.034$ ,  $\chi^2 p = 0.181$ ), very low CBV (AUC 0.71,  $R^2 = 0.249$ ,  $p = 0.026$ ,  $\chi^2 p = 0.382$ ), and severely delayed perfusion (AUC 0.74, Tmax 14 seconds,  $R^2 = 0.372$ ,  $p = 0.011$ ,  $\chi^2 p = 0.071$ ). Next,  $E$  permeability maps at a threshold of 30% were better at predicting PH than ischemic core volume (AUC 0.77,  $R^2 = 0.281$ ,  $p = 0.048$ ,  $\chi^2 p = 0.249$ ), very low CBV (AUC 0.74,  $R^2 = 0.187$ ,  $p = 0.041$ ,  $\chi^2 p = 0.124$ ), reperfusion (AUC 0.75,  $R^2 = 0.182$ ,  $p = 0.037$ ,  $\chi^2 p = 0.131$ ), and severely delayed perfusion (AUC 0.75, Tmax 14 seconds  $R^2 = 0.134$ ,  $p = 0.037$ ,  $\chi^2 p = 0.091$ ). A combined model with an  $E$  map lesion volume at a 30% threshold restricted to within the perfusion lesion and ischemic core volume was also highly accurate at predicting PH (AUC 0.92  $R^2 = 0.488$ ,  $p < 0.001$ ,  $\chi^2 p = 0.291$ ), but not HT (AUC 0.74,  $R^2 = 0.143$ ,  $p = 0.029$ ,  $\chi^2 p = 0.491$ ).

## Discussion

From a large, multicenter, international database, we have shown that permeability maps are a strong imaging predictor of HT, including PH1 and PH2, in ischemic stroke patients treated with intravenous alteplase. Additionally, compared with previously described imaging predictors of hemorrhage,  $E$  permeability was significantly more accurate, sensitive, and specific at predicting hemorrhage. Moreover, the extent of the  $E$  lesion confined within the perfusion lesion was proportional to the severity of hemorrhage across the range of HI1, HI2, PH1, and PH2. Furthermore, the predictive accuracy was very strong, with AUC  $> 0.9$ . Not surprisingly, the  $E$  permeability maps could not predict remote hemorrhage and were able to predict hemorrhages only when they originated within the acute perfusion lesion.

Previously identified markers of HT have insufficient power to alter a treatment decision-making process and have not been implemented in guidelines as contraindications to thrombolysis. The present study provides data to propose a highly accurate predictor of HT likelihood using the  $E$  permeability map at a threshold of 30% within the perfusion deficit. Although the  $E$  permeability map and threshold cannot predict remote hemorrhage, remote hemorrhage is much less common and probably reflects disorders of fibrinogen production. There is the potential that this measure could be used to alter treatment decision-making and, possibly, the consent process. In patients with

a large  $E$  lesion, for example if a patient had a 60% risk of a PH, this information can be used to inform patient family discussions around expected outcomes and decision-making or guide future clinical trials. Additionally,  $E$  permeability measures could be useful in trials of HT or PH prevention to isolate a group of patients at risk and enrich the trial cohort.

Study limitations need to be acknowledged. Firstly, although INSPIRE is a large, multisite study, in which the sites are strongly encouraged to enroll consecutive patients, the need for pretreatment multimodal CT and follow-up MR, along with clinical data from several time points, means that, practically, not all thrombolysed patients at the centers were included.<sup>29</sup> Therefore, despite the known baseline clinical and imaging characteristics, some unknown patient cohort biases might have been present, which we cannot take into account. Secondly, the assessment of the follow-up hemorrhage might have been affected by the use of CT in a proportion of cases, and even in cases with MRI, not all had susceptibility weighted imaging (SWI); therefore, some smaller hemorrhages might have been missed. If a different post-processing algorithm is used to derive the  $E$  measures, then this method would need to be revalidated in a similar manner to the present study; however, the underlying principles are likely to be the same, but might need different thresholds if processed with different algorithms. Importantly, variations in motion correction might also produce different study results, particularly for longer scans, where motion becomes more likely. Next, CTP acquisitions in the present study were of differing lengths ( $\geq 45$  seconds in length, but the majority were  $> 60$  seconds). This might have led to variability in the permeability measures from different centers, particularly for the measures of  $K_{trans}$  and  $PS$ . Lastly, we did not include patients undergoing thrombectomy at the time of the analysis because we were underpowered, and replication to adjust the statistical model is required.

In conclusion, the present study has identified that permeability measures from CTP can accurately predict HT in ischemic stroke patients treated with intravenous alteplase alone. This technique could potentially be useful in trials seeking to target ischemic stroke patients at high risk of HT and might influence the calculation of thrombolysis risk–benefit ratio in individual patients in clinical practice, especially if validated in a thrombectomy cohort.

## Acknowledgments

This study was supported by the National Health and Medical Research Council (grant APP1013719, A.B.), National Health and Medical Research Council/National

Heart Foundation co-funded Career Development/Future Leader Fellowship (grant APPS1110629/100827, N.J.S.), The Science and Technology Commission of Shanghai Municipality China (grants 1241119a8100 and 15QA1400900, X.C.), and The Canada Research Chair Program (K.B.). Dr Aviv is funded by a CIHR project grant 362185.

## Author Contributions

Conception and design of the study: A.B., M.P., C.L., and K.B. Acquisition and analysis of data: all authors. Drafting manuscript and figures: A.B., C.C., and M.P. Revision and approval of manuscript: all authors.

## Potential Conflicts of Interest

Nothing to report.

## References

- Paciaroni M, Agnelli G, Corea F, Ageno W, Alberti A, Lanari A, Caso V, Micheli S, Bertolani L, Venti M, Palmerini F, Biagini S, Comi G, Previdi P, Silvestrelli G Early hemorrhagic transformation of brain infarction: rate, predictive factors, and influence on clinical outcome: results of a prospective multicenter study. *Stroke* 2008; 39: 2249–2256.
- Yaghi S, Eisenberger A, Willey JZ. Symptomatic intracerebral hemorrhage in acute ischemic stroke after thrombolysis with intravenous recombinant tissue plasminogen activator: a review of natural history and treatment. *JAMA Neurol* 2014; 71: 1181–1185.
- Hacke W, Kaste M, Bluhmki E, Brozman M., Dávalos A., Guidetti D., Larrue V., Lees K.R., Medeghri Z., Machnig T., Schneider D., von Kummer R., Wahlgren N., Toni D., ECASS Investigators Thrombolysis with Alteplase 3 to 4.5 hours after acute ischemic stroke. *New Engl J Med* 2008; 359: 1317–1329.
- Group TNiONDaSr-PSS. Tissue plasminogen activator for acute ischemic stroke. *N Engl J Med* 1995; 333: 1581–1587.
- Lees KR, Bluhmki E, von Kummer R, Brott TG, Toni D, Grotta JC, Albers GW, Kaste M, Marler JR, Hamilton SA, Tilley BC, Davis SM, Donnan GA, Hacke W Time to treatment with intravenous alteplase and outcome in stroke: an updated pooled analysis of ECASS, ATLANTIS, NINDS, and EPITHET trials. *Lancet* 2010; 375: 1695–1703.
- Hacke W, Kaste M, Fieschi C, von Kummer R., Davalos A., Meier D., Larrue V., Bluhmki E., Davis S., Donnan G., Schneider D., Diez-Tejedor E., Trouillas P. Randomised double-blind placebo-controlled trial of thrombolytic therapy with intravenous alteplase in acute ischaemic stroke (ECASS II). Second European-Australasian acute stroke study investigators. *Lancet* 1998; 352: 1245–1251.
- Cuenod CA, Balvay D. Perfusion and vascular permeability: basic concepts and measurement in DCE-CT and DCE-MRI. *Diagn Interv Imaging* 2013; 94: 1187–1204.
- Yen P, Cobb A, Shankar JJ. Does computed tomography permeability predict hemorrhagic transformation after ischemic stroke? *World J Radiol* 2016; 8: 594–599.
- Leigh R, Jen SS, Hillis AE, Krakauer JW, Barker PB, Albers GW, Davis SM, Donnan GA, Fisher M, Furlan AJ, Grotta JC, Hacke W, Kang DW, Kidwell C, Koroshetz WJ, Lees KR, Lev MH, Liebeskind DS, Sorensen AG, Thijs VN, Thomalla G, Warach SJ, Wardlaw JM, Wintermark M Pretreatment blood-brain barrier damage and post-treatment intracranial hemorrhage in patients receiving intravenous tissue-type plasminogen activator. *Stroke* 2014; 45: 2030–2035.
- Patlak CS, Blasberg RG. Graphical evaluation of blood-to-brain transfer constants from multiple-time uptake data. *J Cereb Blood Flow Metab* 1985; 5: 584–590.
- Topakian R, Barrick TR, Howe FA, Markus HS. Blood-brain barrier permeability is increased in normal-appearing white matter in patients with lacunar stroke and leucoaraiosis. *J Neurol Neurosurg Psychiatry* 2010; 81: 192–197.
- Tofts PS, Brix G, Buckley DL, Evelhoch JL, Henderson E, Knopp MV, Larsson HBW, Lee TY, Mayr NA, Parker GJM, Port RE, Taylor J, Weisskoff RM Estimating kinetic parameters from dynamic contrast-enhanced T(1)-weighted MRI of a diffusable tracer: standardized quantities and symbols. *J Magn Reson Imaging* 1999; 10: 223–232.
- Horsch AD, Dankbaar JW, van Seeters T, Niesten JM, Luitse MJA, Vos PC, van der Schaaf IC, Biessels GJ, van der Graaf Y, Kappelle LJ, Mali WPTM, Velthuis BK Relation between stroke severity, patient characteristics and CT-perfusion derived blood-brain barrier permeability measurements in acute ischemic stroke. *Clin Neuroradiol* 2016; 26: 415–421.
- Ozkul-Wermester O, Guegan-Massardier E, Triquenot A, Borden A, Perot G, Gérardin E Increased blood-brain barrier permeability on perfusion computed tomography predicts hemorrhagic transformation in acute ischemic stroke. *Eur Neurol* 2014; 72: 45–53.
- Butcher K, Christensen S, Parsons M, de Silva DA, Ebinger M, Levi C, Jeerakathil T, Campbell BC, Barber PA, Bladin C, Fink J, Tress B, Donnan GA, Davis SM, EPITHET Investigators Postthrombolysis blood pressure elevation is associated with hemorrhagic transformation. *Stroke* 2010; 41: 72–77.
- Lansberg MG, Albers GW, Wijman CA. Symptomatic intracerebral hemorrhage following thrombolytic therapy for acute ischemic stroke: a review of the risk factors. *Cerebrovasc Dis* 2007; 24: 1–10.
- Tanne D, Kasner SE, Demchuk AM, Koren-Morag N, Hanson S, Grond M, Levine SR, the Multicenter rt-PA Stroke Survey Group Markers of increased risk of intracerebral hemorrhage after intravenous recombinant tissue plasminogen activator therapy for acute ischemic stroke in clinical practice: the Multicenter rt-PA Stroke Survey. *Circulation* 2002; 105: 1679–1685.
- Derech L, Hermier M, Adeleine P et al. Clinical and imaging predictors of intracerebral haemorrhage in stroke patients treated with intravenous tissue plasminogen activator. *J Neurol Neurosurg Psychiatry* 2005; 76: 70–75.
- Bivard A, Levi C, Spratt N, Parsons M. Perfusion CT in acute stroke: a comprehensive analysis of infarct and penumbra. *Radiology* 2013; 267: 543–550.
- Bivard A, Levi C, Krishnamurthy V, Hislop-Jambrich J, Salazar P, Jackson B, Davis S, Parsons M Defining acute ischemic stroke tissue pathophysiology with whole brain CT perfusion. *J Neuroradiol* 2014; 41: 307–315.
- Campbell BC, Christensen S, Parsons MW, Churilov L, Desmond PM, Barber PA, Butcher KS, Levi CR, de Silva DA, Lansberg MG, Mlynash M, Olivot JM, Straka M, Bammer R, Albers GW, Donnan GA, Davis SM, EPITHET and DEFUSE Investigators Advanced imaging improves prediction of hemorrhage after stroke thrombolysis. *Ann Neurol* 2013; 73: 510–519.
- Yassi N, Parsons MW, Christensen S, Sharma G, Bivard A, Donnan GA, Levi CR, Desmond PM, Davis SM, Campbell BCV Prediction of poststroke hemorrhagic transformation using computed tomography perfusion. *Stroke* 2013; 44: 3039–3043.
- von Kummer R, Broderick JP, Campbell BC et al. The Heidelberg bleeding classification: classification of bleeding events after ischemic stroke and reperfusion therapy. *Stroke* 2015; 46: 2981–2986.
- Bisdas S, Hartel M, Cheong LH, Koh TS, Vogl TJ Prediction of subsequent hemorrhage in acute ischemic stroke using permeability CT imaging and a distributed parameter tracer kinetic model. *J Neuroradiol* 2007; 34: 101–108.

25. Larson KB, Markham J, Raichle ME. Tracer-kinetic models for measuring cerebral blood flow using externally detected radiotracers. *J Cereb Blood Flow Metab* 1987; 7: 443–463.
26. Bisdas S, Donnerstag F, Berding G, Vogl T.J., Thng C.H., Koh T.S. Computed tomography assessment of cerebral perfusion using a distributed parameter tracer kinetics model: validation with H(2)((15))O positron emission tomography measurements and initial clinical experience in patients with acute stroke. *J Cereb Blood Flow Metab* 2008; 28: 402–411.
27. Kellogg GE, Fornabaio M, Chen DL, Abraham DJ, Spyraakis F, Cozzini P, Mozzarelli A Tools for building a comprehensive modeling system for virtual screening under real biological conditions: the computational titration algorithm. *J Mol Graph Model* 2006; 24: 434–439.
28. Jain R, Ellika SK, Scarpace L, Schultz LR, Rock JP, Gutierrez J, Patel SC, Ewing J, Mikkelsen T Quantitative estimation of permeability surface-area product in astroglial brain tumors using perfusion CT and correlation with histopathologic grade. *AJNR Am J Neuroradiol* 2008; 29: 694–700.
29. Cereda CW, Christensen S, Campbell BCV, Mishra NK, Mlynash M, Levi C, Straka M, Wintermark M, Bammer R, Albers GW, Parsons MW, Lansberg MG A benchmarking tool to evaluate computer tomography perfusion infarct core predictions against a DWI standard. *J Cereb Blood Flow Metab* 2016; 36: 1780–1789.